2nd-Harmonic generation in purple membrane-poly(vinyl alcohol) films—probing the dipolar characteristics of the bacteriorhodopsin chromophore in BR570 and M412

ARTICLE *in* THE JOURNAL OF PHYSICAL CHEMISTRY · APRIL 1989

Impact Factor: 2.78 · DOI: 10.1021/j100345a086

3 AUTHORS, INCLUDING:

Jung Y. Huang
Chiao Tung University
125 PUBLICATIONS **1,939** CITATIONS

SEE PROFILE

Second-Harmonic Generation in Purple Membrane–Poly(vinyl alcohol) Films: Probing the Dipolar Characteristics of the Bacteriorhodopsin Chromophore in bR_{570} and M_{412}

Jung Y. Huang, Zhongping Chen, and Aaron Lewis*,†

Department of Applied Physics, Clark Hall, Cornell University, Ithaca, New York 14853
(Received: February 4, 1988; In Final Form: July 6, 1988)

The second-order nonlinear optical properties of purple membrane–poly(vinyl alcohol) films (PM–PVA) are investigated by second-harmonic generation. The magnitudes and the phases of the second-order molecular polarizabilities of the bacteriorhodopsin molecule in the bR_{570} and M_{412} states are obtained. Comparing these results with those obtained for free retinal and retinal Schiff bases spread at air–water interfaces indicates that, upon electronic excitation, the dipole moment change of the retinylidene chromophore in bR_{570} appears larger than for the chromophore when it is not complexed to the protein. The observed second-harmonic signal from a PM–PVA film bleached by a CW light source agrees well with the square of the calculated mole fraction of the bR_{570} intermediate. The implications of our findings are discussed.

Introduction

Bacteriorhodopsin (bR) is a unique energy transducing molecule that is the only protein found in the purple membrane which grows in the bacterium *Halobacterium halobium*.[1] The physiological role of this molecule is to convert light energy into a proton gradient across the bacterial cell membrane. The initial step in this process of photoactivated proton pumping is the absorption of light by the retinylidene chromophore which is embedded and covalently attached to a protein matrix to form the bacteriorhodopsin molecule. Several investigations have shown that the photochemical event initiated by this photon absorption is completed within less than a picosecond.[2,3] During this time scale of several hundred femtoseconds (450 fs), 30% of the photon energy is stored and activates the pumping of a proton. The mechanism of this energy storage in retinylidene proteins remains a major unresolved problem in biophysics. It is clear that a primary step in understanding this mechanism is a detailed investigation of transient electronic changes induced by the absorption of a photon. The polarizability and alterations in dipole moment of a molecule are two indicators of light-induced changes in molecular electronic structure. Although these parameters can be measured for a molecule in solution by using an electrochromic technique,[4] such electronic properties of a chromophore embedded in a protein matrix are most difficult to determine with this method.

In this paper, we report on our studies of these electronic properties of the bR molecule using second-harmonic generation (SHG). Second-harmonic generation is the lowest order nonlinear optical process, in which the second-order polarizability of a material is responsible for the generation of light at the second-harmonic frequency. Due to symmetry considerations, SHG is forbidden in an isotropic medium in the electric dipole approximation. Inspired by the ingenious work of Y. R. Shen's group,[5] SHG has been successfully applied to many fields[5-10] and much information has been gained. However, there have been few attempts to apply SHG to biological systems.[11,12] Membranes are biological systems that contain naturally oriented dipole layers. The dipole layers of purple membrane can also be readily oriented in polymer matrices and electric fields. Thus, the purple membrane provides an important and ideal system to which SHG can be applied and can give unique information on the electronic properties of this system which has not been possible to obtain by any other method.

Experimental Section

A Q-switched frequency-doubled Nd:YAG laser with a 10-Hz repetition rate and 10-ns pulse-width was used. The Nd:YAG laser was adjusted to give an infrared 1064-nm beam of less than 60 mW which was focused onto a 3.5-mm-diameter spot on the sample surface. The infrared nature of the fundamental beam is specifically important in reducing damage and preventing bleaching of the bR molecules. The transmitted (or reflected) SH photons at 532 nm were detected by a cooled RCA C31034 photomultiplier tube and averaged by a boxcar integrator. The detailed setup has been described previously.[13]

Our detection sensitivity was calibrated against the second-harmonic intensity from a 1.196-mm-thick x-cut quartz plate. The quartz plate was rotated 29° about the y axis of the crystal to obtain one of the maxima of the Maker fringes. The polarizations of the fundamental and second-harmonic beams were chosen to be p-polarized relative to the plane of incidence. Using the known nonlinear second-order susceptibility $\chi^{(2)}_{zzz} = 1.9 \times 10^{-9}$ esu[14] and the index of refraction of the quartz crystal at 1064 and 532 nm,[15] we obtained a ratio of[16]

$$I_{p\rightarrow p}(2\omega)/[I_p(\omega)]^2 = 1.5 \times 10^{-25}\ \mathrm{cm^2/erg} \qquad (1)$$

The phase of the second-order nonlinear optical susceptibility is determined from a scheme reported by Kemnitz et al.[17] The

† Please address reprint requests to Division of Applied Physics, The Hebrew University of Jerusalem, Jerusalem, Israel.

(1) For a review see: *Methods in Enzymology*; Packer, L. P., Ed.; Academic: New York, 1982; Vol. 88, Part I.
(2) (a) Ippen, E.; Shank, C. V.; Lewis, A.; Marcus, M. *Science* **1978**, *200*, 1279. (b) Downer, M. C.; Islam, M.; Shank, C. V.; Harotunian, A.; Lewis, A. In *Ultrafast Phenomena IV*; Austin, D. H., Eisenthal, K. B., Eds.; Springer-Verlag: Berlin, 1984.
(3) (a) Polland, H. J.; Franz, M. A.; Zenith, W.; Kaiser, W.; Kolling, E.; Oesterhelt, D. *Biophys. J.* **1986**, *49*, 65. (b) Mathies, R. A.; Brito Cruz, C. H.; Pollard, W. T.; Shank, C. V. *Science* **1988**, *240*, 777.
(4) (a) Mathies, R.; Stryer, L. *Proc. Natl. Acad. Sci. U.S.A.* **1976**, *73*, 2169. (b) Ponder, M.; Mathies, R. *J. Phys. Chem.* **1983**, *87*, 5090.
(5) Shen, Y. R. *Annu. Rev. Mater. Sci.* **1986**, *16*, 69.
(6) Akhmanov, S. A.; Emel'yanov, V. I.; Koroteev, N. I.; Seminogov, V. N. *Sov. Phys.—Usp. (Engl. Transl.)* **1986**, *28*, 1084.
(7) Berkovic, G.; Rasing, Th.; Shen, Y. R. *J. Chem. Phys.* **1986**, *85*, 7374.
(8) Richmond, G. L. *Surf. Sci.* **1984**, *147*, 115.
(9) Hicks, J. M.; Kemnitz, K.; Eisenthal, K. B.; Heinz, T. F. *J. Phys. Chem.* **1986**, *90*, 560.
(10) Bhattacharyya, K.; Sitzmann, E. V.; Eisenthal, K. B. *J. Chem. Phys.* **1987**, *87*, 1442.
(11) Freund, I.; Deutsch, M.; Sprecher, A. *Biophys. J.* **1986**, *50*, 693.
(12) Aktsipetrov, O. A.; Akhmediev, N. N.; Vsevolodov, N. N.; Esikov, D. A.; Shutov, D. A. *Sov. Phys.—Dokl. (Engl. Transl.)* **1987**, *32*, 219.
(13) Huang, J. Y.; Lewis, A.; Rasing, Th. *J. Phys. Chem.* **1988**, *92*, 1756.
(14) Shen, Y. R. *The Principle of Nonlinear Optics*; Wiley: New York, 1984; p 101.
(15) Philipp, H. R. *Handbook of Optical Constants of Solids*; Palik, E. D., Ed.; Academic: New York, 1985; pp 719–747.
(16) Jerphagnon, J.; Kurtz, S. K. *J. Appl. Phys.* **1970**, *41*, 1667. Our $\chi^{(2)}$ is according to ref 14.
(17) Kemnitz, K.; Bhattacharyya, K.; Hicks, J. M.; Pinto, G. R.; Eisenthal, K. B.; Heinz, T. F. *Chem. Phys. Lett.* **1986**, *131*, 285.

0022-3654/89/2093-3314$01.50/0

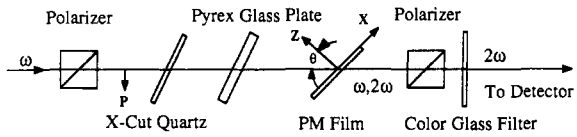

Figure 1. Experimental arrangement for the measurement of the phase of the nonlinear optical susceptibility.

experimental arrangement for this measurement is depicted in Figure 1. Two second-harmonic sources are shown in this figure. One of these sources is the x-cut quartz crystal plate, and the other is the purple membrane thin film. The SH electric fields generated by these two sources will have a definite phase relationship with respect to each other, as each has a specific relationship to the phase of the fundamental field squared.[18] Between these two SH sources, a 3.1-mm-thick Pyrex glass plate was inserted to modulate their relative phase. In our experiment, the distance between the x-cut quartz crystal plate and the purple membrane thin film was fixed to be 19.09 cm.

The purple membrane (PM) was harvested and purified from a fresh batch of *Halobacterium halobium* (S9) according to an established proceudre.[19] Five grams of poly(vinyl alcohol) (PVA, molecular weight 40 000), purchased from Sigma, was dissolved in a 25 mL of 0.1 M Hepes buffer by boiling.[20] As the PVA solution was cooled to room temperature, a small quantity of highly concentrated purple membrane suspended in the same 0.1 M Hepes buffer was added to obtain an aqueous purple membrane–PVA solution with the resultant optical density at 566 nm near 1. The purple membrane–PVA solution was then degassed to remove any residual bubbles.

To make a film, 4 mL of the purple membrane–PVA solution was spread on a leveled glass plate with a diameter of 5 cm. During the drying process, passing filtered air uniformly over the film surface was found to be helpful in forming films with good homogeneity and flatness.

Our film samples were typically 180–210 μm thick, and the optical density at 566 nm was close to 0.18. The drying time for these films normally took 10 h. The absorption spectra of such films show no detectable deviation from that of the purple membrane suspended in a pH 7 buffered solution.

Monolayers at an air–water interface were prepared by using a Langmuir trough. Detailed information about the characteristics of *all-trans*-retinal (ATR), unprotonated butylamine-retinylidene Schiff base (NRB), and protonated butylamine-retinylidene Schiff base (N^+RB–HCl) monolayers has been reported elsewhere.[13]

Theoretical Considerations

(*a*) *The Polarization Dependence of the Transmitted Second-Harmonic Intensity.* The theory of SHG from a thin film is well-established.[16,21] In this paper, we investigate the second-harmonic response of uniaxially oriented samples. Such situations are frequently encountered in adsorbate systems on noncrystalline substrates[5] or in chromophores embedded in polymer matrices.[22] Our purple membrane–PVA films (PM–PVA) are characterized by the substrate normal (z axis) around which the films are rotationally invariant. The xy plane is chosen to be on the film surface with the y axis perpendicular to the plane of incidence. As a result of the rotational invariance, the only two independent components of $\chi^{(2)}$ are $\chi^{(2)}_{zzz}$ and $\chi^{(2)}_{xzx}$. The polarization of the second harmonic, therefore, has the form

$$P_x^{2\omega} = \chi^{(2)}_{xzx}E_x^{\omega}E_z^{\omega}$$

$$P_y^{2\omega} = \chi^{(2)}_{xzx}E_z^{\omega}E_y^{\omega}$$

$$P_z^{2\omega} = \chi^{(2)}_{zzz}E_z^{\omega}E_z^{\omega} + \chi^{(2)}_{zxx}E_x^{\omega}E_x^{\omega} + \chi^{(2)}_{zxx}E_y^{\omega}E_y^{\omega} \quad (2)$$

where $\chi^{(2)}_{ijk}$ is the nonlinear optical susceptibility and $E^{\omega}_{x,y,z}$ are the electric fields along the directions of the x, y, or z axes inside the film. With the incident laser light p-polarized, the transmitted p-polarized SH intensity is a function of the angle (θ) between the incident fundamental beam and the film normal and is given by[16]

$$I_{p\to p}(2\omega)/[I_p(\omega)]^2 = \frac{32\pi^3}{c}|\chi^{(2)}_{zzz}|^2 T^p_{2\omega} p_1^2(\theta)\frac{\sin^2\Psi(\theta)}{(n_\omega^2 - n_{2\omega}^2)^2} \quad (3)$$

where $T^p_{2\omega}$ is the Fresnel-like transmission factor when the nonlinear polarization $P^{2\omega}$ is in the plane of incidence, the n's are the refractive indexes at the indicated frequencies, and $\Psi(\theta)$ is the angular dependence of the second-harmonic power resulting from interference between free and bound waves. $p_1(\theta)$ is a projection factor that depends on the form of the nonlinear susceptibility tensor, $\chi^{(2)}$, and on the direction of $P^{2\omega}$ compared with the plane of incidence. With the indicated film symmetry and the electric polarizations, we have

$$p_1(\theta) = [\eta\cos^2\theta_\omega \sin\theta_\omega + (\sin\theta_\omega)(\eta\cos^2\theta_\omega + \sin^2\theta_\omega)](t^p_\omega)^2 \quad (4)$$

where $\eta = |\chi^{(2)}_{xzx}|/|\chi^{(2)}_{zzz}|$, θ_ω is the refractive angle of the fundamental beam, and t^p_ω is the Fresnel transmission factor for the p-polarized fundamental electric field. For retinylidene molecules for which the second-order molecular polarizability $\alpha^{(2)}$ is dominated by a single axial component $\alpha^{(2)}_{\zeta\zeta\zeta}$, the nonvanishing components of $\chi^{(2)}$ are given by[5]

$$(\chi^{(2)})_{zxx} = (\chi^{(2)})_{xzx} = (\chi^{(2)})_{xxz} = \tfrac{1}{2}N\langle\cos\zeta\sin^2\zeta\rangle\alpha^{(2)}_{\zeta\zeta\zeta}$$

$$(\chi^{(2)})_{zzz} = N\langle\cos^3\zeta\rangle\alpha^{(2)}_{\zeta\zeta\zeta} \quad (5)$$

where ζ is the angle between the molecular ζ axis and the film normal. For other polarization arrangements, the transmitted SH intensities are summarized as follows:

$$I_{s\to p}(2\omega)/[I_p(\omega)]^2 = \frac{32\pi^3}{c}|\chi^{(2)}_{zzz}|^2 T^p_{2\omega} p_2^2(\theta)\frac{\sin^2\Psi(\theta)}{(n_\omega^2 - n_{2\omega}^2)^2} \quad (6)$$

$$I_{45^\circ\to p}(2\omega)/[I(\omega)]^2 = \frac{32\pi^3}{c}|\chi^{(2)}_{zzz}|^2 T^p_{2\omega} p_3^2(\theta)\frac{\sin^2\Psi(\theta)}{(n_\omega^2 - n_{2\omega}^2)^2} \quad (7)$$

$$I_{45^\circ\to s}(2\omega)/[I(\omega)]^2 = \frac{32\pi^3}{c}|\chi^{(2)}_{zzz}|^2 T^s_{2\omega} p_4^2(\theta)\frac{\sin^2\Psi(\theta)}{(n_\omega^2 - n_{2\omega}^2)^2} \quad (8)$$

$$I_{s\to s}(2\omega) = I_{p\to s}(2\omega) = 0 \quad (9)$$

where $p_2(\theta) = \eta(t^s_\omega)^2\sin\theta_\omega$, $p_3(\theta) = 0.5\eta\cos^2\theta_\omega\sin\theta_\omega\,(t^p_\omega)^2 + 0.5\sin\theta_\omega\,[(t^p_\omega)^2\sin^2\theta_\omega + \eta(t^p_\omega)^2\cos^2\theta_\omega + \eta(t^s_\omega)^2]$, and $p_4(\theta) = 0.5\eta(t^s_\omega t^p_\omega)\sin\theta_\omega$.

(*b*) *Self-Absorption Effect.* If the film has absorption losses at both the fundamental and harmonic frequencies, the above equations should be modified to reflect these losses.[18] Normally, the optical attenuation of a thin film, $\epsilon = \epsilon(2\omega) - 2\epsilon(\omega)$, is much smaller than the dispersion that it induces, i.e., $\epsilon/2 \ll k(2\omega) - 2k(\omega)$. Under this condition, the self-absorption can be corrected by simply replacing the $\sin^2\Psi(\theta)$ of eq 3, 6, 7, and 8 with $0.25(1 - e^{-\epsilon l}) + e^{-\epsilon l}\sin^2\Psi(\theta)$, where l is the thickness of the film.

(*c*) *Phase Determination.* The interference pattern obtained from the experimental setup which is shown in Figure 1 can be expressed as[23]

$$I = I_Q + I_s + 2I_Q^{1/2}I_s^{1/2}\cos\Delta \quad (10)$$

where Δ is the relative phase delay between the two SH electric fields and can be further expressed as

$$\Delta = (\gamma_s - \gamma_Q) + D_A + D_G(\phi) + D_Q(\delta) + D_s \quad (11)$$

with

(18) Wynne, J. J.; Bloembergen, N. *Phys. Rev.* **1969**, *188*, 1211.
(19) Oesterhelt, D.; Stoeckenius, W. *Methods in Enzymology*; Packer, L. P., Ed.; Academic: New York, 1974; Vol. 31, Part A, p 667.
(20) Teng, T. Y.; Huang, H. W. *Biochim. Biophys. Acta* **1986**, *874*, 13.
(21) Bloembergen, N.; Pershan, P. S. *Phys. Rev.* **1962**, *128*, 606.
(22) Singer, K. D.; Sohn, J. E.; Lalama, S. J. *Appl. Phys. Lett.* **1986**, *49*, 248.
(23) Velsko, S. P.; Eimerl, D. *Appl. Opt.* **1986**, *25*, 1344.

$$\chi_s^{(2)} = |\chi_s^{(2)}|e^{i\gamma_s}$$

$$\chi_Q^{(2)} = |\chi_Q^{(2)}|e^{i\gamma_Q}$$

$$D_A = 2\omega[n_a(\omega) - n_a(2\omega)]L_a/c$$

$$D_G(\phi) = (2\omega L_g/c)[n_g(\omega)/\cos\phi_\omega - n_g(2\omega)/\cos\phi_{2\omega}]$$

$$D_Q(\delta) = 0.5\pi[1 - L_Q/l_{coh}^Q(\delta)] \qquad (12)$$

Here γ_Q and γ_s are the phase factors of the second-order nonlinear susceptibilities of the x-cut quartz crystal plate and the thin film sample; D_A and $D_G(\phi)$ are the dispersions between the fundamental and the SH frequencies, which are induced by air and the Pyrex glass plate; and D_Q (or D_s) is the phase difference between the SH electric field generated from the quartz crystal (or the thin film sample) and the incident fundamental field squared. This phase delay factor depends on the thickness, L_Q, and the coherent length, l_{coh}^Q, of the plate. L_a and L_g in eq 12 are the path length in air and the thickness of the Pyrex glass plate. The propagation angles of the fundamental and the SH beams in the Pyrex glass plate are determined by Snell's law and are indicated by ϕ_ω and $\phi_{2\omega}$, respectively. With the known indexes of refraction of air, Pyrex glass, and quartz crystal, the phase factor of the nonlinear susceptibility of the sample, γ_s, can be determined from the interference pattern.

Results

(a) *Origin of the SHG from PM–PVA Films.* PM–PVA films are complicated systems. Many groups inside the films could participate in the generation of the SH signal. Among these probable SH sources, the retinal chromophore has the largest second-order molecular polarizability.[13] However, in view of the diluteness of the retinal chromophore in the PM–PVA films, the SH signal generated by the chromophore may be negligible. To identify the role of the retinal in the SHG, the relationship between the SH signal from the PM–PVA films and the photochemistry of bacteriorhodopsin has to be established.

The bR photochemistry is initiated when the retinal chromophore absorbs a photon with wavelength around 570 nm. A single-photon absorption transforms in 0.4 ps the initial state bR_{570} (maximum of absorption $\lambda_{max} \simeq 570$ nm) into an intermediate J_{650} with an absorption maximum at ≃650 nm. The J_{650} species thermally transforms in 3 ps into the intermediate K_{610}, which in turn thermally generates the L species. Finally, after a series of progressively longer lived intermediates bR_{570} is thermally regenerated to produce a photon-induced cycle of events (see Figure 2).

It is well-established[24] that if the purple membrane is illuminated with an argon ion laser at 5145 or 4579 Å, a photostationary state is established in which a large fraction of the bR_{570} molecules are transformed to the M_{412} intermediate which absorbs at 412 nm. The SH photons generated by illuminating the purple membrane with a Nd:YAG laser are at 532 nm, and this is in resonance with bR_{570} and not M_{412}. Therefore, it would be expected that if the retinal chromophore played a dominant role in generating the SH signal from PM–PVA films, then this SH signal would be seriously perturbed by illuminating the PM–PVA film with argon ion laser wavelengths at 5145 or 4579 Å. In order to verify this notion, the steady-state concentrations of the bR intermediates during the SH measurement were varied by illuminating the PM–PVA film with a CW argon ion laser at the above wavelengths. The results of the SH measurements under different bleaching conditions are shown in Figure 3a. In this figure, the open circles are the observed SH intensities from a PM–PVA film which is continuously illuminated by a 5145-Å argon ion laser. The filled circles in this figure indicate the SH intensities when the wavelength of the bleaching light is 4579 Å.

If the 5145-Å laser line is used as the bleaching light cycle the SH intensity rapidly decreases with the bleaching laser intensity to about 10% of the unbleached value and then levels off. The break point roughly occurs when the intensity of the 5145-Å light is 50 mW/cm². For 4579 Å, similar behavior is observed. However, the light intensity at the break point is smaller than that for 5145 Å. Also, with this wavelength, the SH intensity decreases to only 70% of its unbleached value.

The bR_{570} mole fraction is calculated by using the bR photochemical cycle shown in Figure 2 as our model. The solid line in Figure 3a indicates the square of the calculated mole fraction of bR_{570} as a function of the laser intensity at 5145 Å. The dashed line represents the calculated result for 4579 Å. The mole fractions

(24) Goldschmidt, C. R.; Ottolenghi, M.; Korenstein, R. *Biophys. J.* **1976**, *16*, 839.

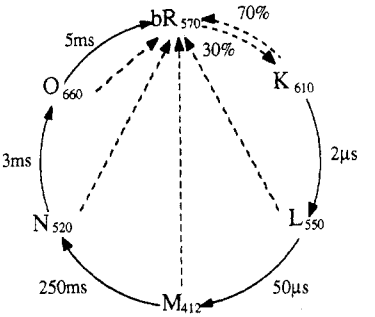

Figure 2. Photochemical cycle of the bacteriorhodopsin (bR) molecule. The thermal decay path for every intermediate is shown by solid arrows. The dashed arrows indicate photon-driven processes.

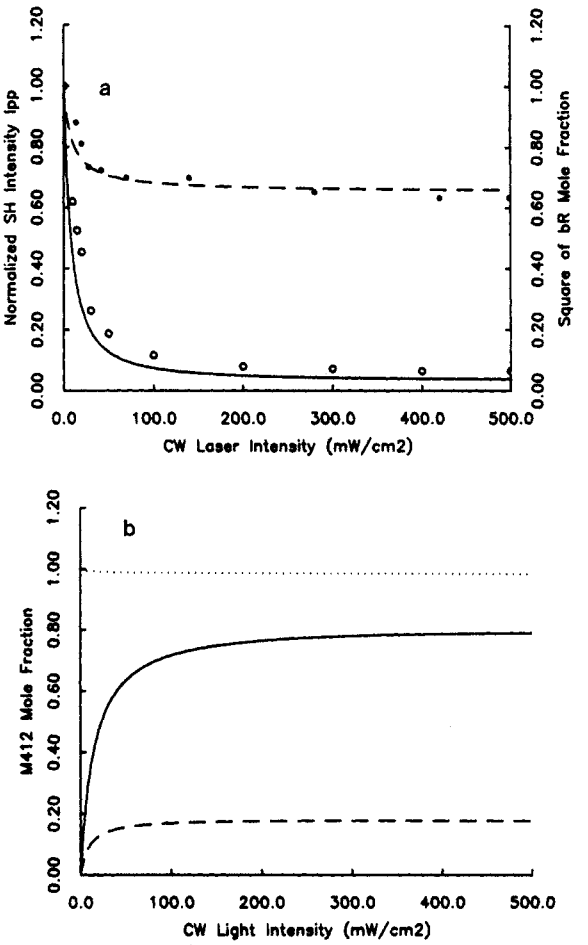

Figure 3. (a) Second-harmonic (SH) intensity, $I_{p\to p}(2\omega)$, from a bleached purple membrane–poly(vinyl alcohol) film (PM–PVA). The open circles are the data from a PM–PVA film bleached by a 5145-Å CW argon ion laser, while the filled circles represent the case in which a 4579-Å CW light source is used. The solid and the dashed lines represent the square of the calculated mole fraction of bR_{570} for 5145- and 4579-Å bleaching light sources, respectively. (b) Calculated mole fraction of M_{412} at two different bleaching wavelengths. The solid line indicates the case when a 5145-Å laser line is used. The result for the 4579-Å laser is shown by the dashed line. The summation of the mole fractions of bR_{570} and M_{412} for the 5145-Å bleaching light is represented by the dotted line.

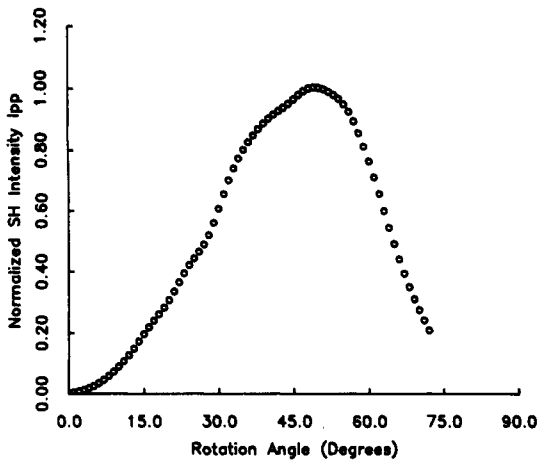

Figure 4. Angular dependence of the transmitted SH intensity, $I_{p\to p}(2\omega)$, from a 238-μm-thick PM–PVA film. The x axis indicates the angle between the incident excitation beam and the film normal.

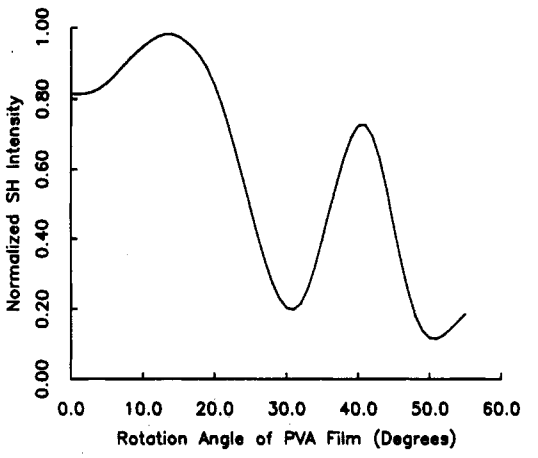

Figure 5. SH interference pattern generated by a quartz crystal and a PM–PVA film. The experimental arrangement used to obtain this data is the same as in Figure 1 except that the Pyrex glass is replaced by a 445-μm-thick PVA film. The x axis indicates the rotation angle of the PVA film.

of the M_{412} intermediate for these two bleaching wavelengths are plotted in Figure 3b.

It is interesting to note that the square of the calculated mole fraction of bR_{570} fits the SH data quite well. This can be understood by noting that the observed SH intensity is proportional to the absolute square of the total nonlinear optical susceptibility, $\chi^{(2)}$, which is summed over all the bR photochemical intermediates in the photostationary state. For the decay constants shown in Figure 2, only bR_{570} and M_{412} can be significantly populated. This can be seen from the dotted line in Figure 3b, which is the summation of the calculated mole fractions of bR_{570} and M_{412}. The expression for the resultant SH intensity is then given by

$$I(2\omega) \propto |C_R\chi_R^{(2)} + C_M\chi_M^{(2)}|^2 \qquad (13)$$

where C_R and C_M are the mole fractions of bR_{570} and M_{412}. The similarity of the calculated curve and the SH data indicates that the retinal chromophore indeed plays a dominant role in the SHG and that the magnitude of $\chi_M^{(2)}$ is much smaller than that of $\chi_R^{(2)}$. Therefore, this is consistent with the notion that the presence of the bR_{570} species resonantly enhances the SH signal generated as a result of shining 1.06-μm laser light on a PM–PVA film.

(*b*) *Determination of the Coherence Length in PM–PVA Films.* In order to analyze the SH signal from PM–PVA films, it is important to determine the dispersion parameter $\Delta n = (n_{2\omega} - n_\omega)$, which is included in eq 3. To deduce this parameter, it is necessary to evaluate the coherence length of the PM–PVA film. The transmitted p-polarized SH beam, $I_{p\to p}(2\omega)$, from a 238-μm-thick PM–PVA film as a function of the angle (θ) between the incident p-polarized fundamental beam and the film normal is shown in Figure 4. Although the visibility of the Maker fringes is poor, three inflections in the curve are still observable in this figure. This indicates that the coherence length of the film is much smaller than the thickness.

A more accurate determination of the coherence length can be obtained with an experimental arrangement similar to that shown in Figure 1. The only difference from Figure 1 is that the Pyrex glass plate is replaced by a 445-μm-thick PVA film. By rotating the PVA film, we can obtain the interference pattern of the SH electric fields obtained from the x-cut quartz crystal and the PM–PVA film. This interference pattern is shown in Figure 5. The value of the index of refraction of the PVA film at 1.064 μm was taken to be 1.65.[25] With the positions of the interference maxima and minima in Figure 5 and also with the help of eq 10–12, the dispersion parameter of the PVA film, $\Delta n = (n_{2\omega} - n_\omega)$, was determined to be 0.014 ± 0.0006. This value corresponds to 18 ± 1 μm for the coherence length of the film.

(*c*) *Determination of Average Chromophore Orientation.* Since the second-order molecular polarizability is related to the nonlinear surface susceptibility by a transformation that requires knowledge of the average chromophore orientation, it is necessary to determine this orientation for further analysis of the SH signal. Information on this orientation can be obtained from the polarization dependence of the surface second-harmonic generation.[26] To determine the value of this parameter, the excitation light was chosen to be s-, p-, and 45°-polarized relative to the incident plane. The beam was incident on the sample at an angle of 45° from the surface normal. By adjusting the SH polarization analyzer, we determined the polarization properties of the transmitted SH signal from a 238-μm-thick PM–PVA film. The results are summarized in Table I, where the experimental data and the corresponding calculated values are compared. With eq 3–9 and the n_ω and Δn of the PVA film, we deduced a value of 30° for the inclination angle of the retinal chromophore relative to the film normal. Note (see Table I) that the much weaker s-polarized SH signal supports our assumption that the PM–PVA film is rotationally invariant.[27]

TABLE I: Polarization Dependence of the Transmitted Second-Harmonic Intensity from a Purple Membrane–PVA Film

polarization		$I(2\omega)/I_{p\to p}(2\omega)$	
1.06 μm	0.532 μm	exptl[a]	calcd[b]
p	p	1	1
45°	p	0.44	0.44
s	p	0.12	0.11
p	s	0.06	0
s	s	0.06	0

[a] The thickness and the optical density, OD_{566}, of the film are 238 μm and 0.2108. [b] The transition moment of the excited chromophore is assumed to be 30° away from the substrate normal. The values of the index of refraction of the film at the fundamental and SH frequencies are taken to be 1.65 and 1.6647.

It should be pointed out that eq 3–9 are based on the Kleinman conjecture (i.e., $\chi_{zxx}^{(2)} = \chi_{xzx}^{(2)}$). Although the Kleinman conjecture is valid only for a nonabsorbing material whose nonlinearity originates from the nonlinear response of the electronic system, the equality of $\chi_{zxx}^{(2)} = \chi_{xzx}^{(2)}$ is still applicable to our PM–PVA films. This can be understood by considering the fact that our PM–PVA films are composite systems with the PM fragments embedded in a PVA polymer matrix. This is quite different from the systems that Kleinman considered. Also, of considerable importance in our system is the fact that the second-order molecular polarizability tensor of the retinylidene chromophore in the PM fragments is nearly one-dimensional with the direction along the chromophore's long axis. For an isotropic host material such as the unstretched

(25) Henniker, C. J. *Macromolecules* **1973**, *6*, 514.

(26) Heinz, T. F.; Tom, H. W. K.; Shen, Y. R. *Phys. Rev. A* **1983**, *28*, 1883.

(27) Mazely, T. L.; Hetherington III, W. M. *J. Chem. Phys.* **1987**, *86*, 3640.

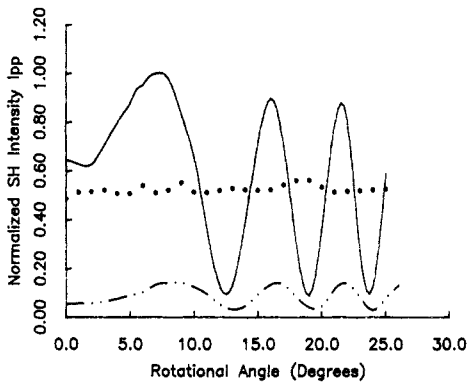

Figure 6. SH interference pattern of the quartz crystal and the PM–PVA film. The x axis indicates the incident angle of the exciting laser beam on the surface of the Pyrex glass plate. The result for the unbleached PM–PVA film is shown by the solid line. When the film is bleached by 100 mW/cm^2 5145-Å light, the SH intensity is shown by the dashed-dot-dot curve. The filled circles indicate the SH output when the PM–PVA film is removed.

PVA films, the one-dimensional characteristics of the second-order molecular polarizability can significantly simplify the transformation matrix which is from the molecular frame to the substrate's frame and leads to the equality of $\chi^{(2)}_{zxx} = \chi^{(2)}_{xzx}$, as can be seen in eq 5.

From the above polarization dependence of the transmitted SH signal of a PM–PVA film, we deduce a value of 30° for the inclination angle of the retinylidene chromophore relative to the film normal. The angle between the polyene chain of the retinal chromophore and the PM surface has been investigated previously by using neutron scattering,[28] polarized Fourier transform infrared difference spectroscopy,[29] and electrodichroism.[30] All these techniques have yielded similar results with a value of 23° for this angle. On the basis of this finding, our data on the chromophore orientation indicate that the planes of the PM fragments make a 53° angle with the substrate normal. Therefore, these results together with the observation of a SH signal clearly indicate that the PM is indeed oriented in the PVA matrix. It is not clear as to the exact nature of the interaction that orients the PM fragments in this matrix. Possibly, the more negative cytoplasmic side[31] of the PM induces a dipolar interaction between the permanent dipole moment of the PM and the polarizable groups in the PVA film. This interaction, which is orientation dependent, could create occupation sites with similar local environment for the PM and, thus, tends to orient the PM fragments to a specific direction.

(d) Determination of the Phase of $\chi^{(2)}_R$. The bleached PM–PVA films used in this study are composed partially of bR_{570} molecules. In order to obtain the absolute contribution of the M_{412} species, the effect of the bR_{570} molecules has to be determined and subtracted out. To accomplish this, one needs to determine the phase of $\chi^{(2)}_R$, the nonlinear susceptibility of bR_{570}, since the SH frequency in our experiments (532 nm) is within the absorption band of bR_{570}, making $\chi^{(2)}_R$ complex.

The experimental arrangement for the measurement of the phase of the nonlinear susceptibility is described in Figure 1. As seen in the Experimental Section, the total SH intensity versus the rotational angle of the Pyrex glass plate will exhibit an interference pattern. These fringes for a PM–PVA film are plotted in Figure 6. In this figure, the solid line indicates the interference of the SH electric field from the PM–PVA film with that from the x-cut quartz crystal. The curve with the filled circles represents the observed SH intensity when the PM–PVA film is removed. Since dispersion in air is not negligible, the distance between the quartz and the PM–PVA film was measured accurately. This distance was chosen to be 19.09 cm in our setup. By substituting the known indexes of refraction of air and Pyrex into eq 12, we can determine the phase angle of $\chi^{(2)}_R$. This parameter, however, depends on the phase angle, γ_Q, of the nonlinear susceptibility of the quartz crystal. By using 180° for γ_Q,[17] a value of 27 ± 8° is deduced for γ_R, the phase angle of the nonlinear susceptibility of the bR_{570} species.

The same measurement was also performed on a bleached PM–PVA film. In this experiment, the bleaching light source was the 5145-Å CW argon ion laser. As shown in Figure 3a, the SH signal from a bleached sample is about 10% of the unbleached value. In order to generate a SH electric field from the quartz crystal with an intensity comparable to that from the bleached sample, the quartz plate is rotated 2° away from the first maximum of the Maker fringes. The interference pattern of the bleached PM–PVA film is shown by the dashed-dot-dot curve in Figure 6. Note that the 2° rotation of the quartz crystal plate can only account for the shift of the interference pattern of the bleached sample by 0.12°. However, by comparison of the solid line with the dashed-dot-dot line in Figure 6, a value of 0.6° is found. Our measurements indicate a value of 0° for γ_M, the phase angle of the M_{412} component of the sample, and this is in agreement with the fact that M_{412} is nonabsorbing at both the fundamental and SH frequencies.

The method for the phase measurement that we used is described in Figure 1 and is very similar to that proposed by Kemnitz et al.[17] However, a slight modification was made in this procedure in order to meet our needs. In the Kemnitz et al. scheme, a quartz crystal plate is translated more than 22 mm to obtain one period of the interference pattern between the SH electric field of the thin film sample and the quartz crystal plate. This procedure may induce significant signal variation and could bury the interference pattern if the excitation laser is not highly collimated. In our procedure, we keep the distance between the quartz crystal plate and the thin film sample constant and a Pyrex glass plate is inserted between these two SH sources to modulate their relative phase. This method works well even when a focused (noncollimated) excitation beam is used.

The measurement of the absolute phase of the surface SH light field can refine our determination of the chromophore orientation discussed above. Inspired by the work of Kemnitz et al.,[17] we have applied the methodology shown in Figure 1 to further investigate the orientational property of the retinal chromophores in the PM–PVA films. The interference pattern obtained from a PM–PVA film with one of the surfaces facing the incident excitation beam is compared with the same film rotated by 180°. (No glass substrate is involved in this measurement.) We have observed a 180° phase shift between the interference patterns generated by these two orientations of the film. This can be understood by considering this effect of 180° rotation as being the same as an inversion operation performed on the chromophores, which results in a change in sign of the nonlinear susceptibility seen in eq 5. It is interesting to point out that the interference pattern of the PM–PVA film with the upper surface of the film facing the incoming excitation beam is similar to that obtained from a N^+RB–HCl monolayer that is spin-coated on a glass surface and is oriented such that the monolayer is facing the beam. Considering that the Schiff base nitrogen is the most hydrophilic part of the N^+RB–HCl molecule, it is expected that it is this atom which contacts with the native hydrophilic glass surface. The similarity in these two interference patterns indicates that the β-ionone ring of the bound retinylidene chromophore in the PM–PVA film points away from the substrate as it does in the N^+-RB–HCl monolayer. Our results unambiguously show that the retinal chromophores in the PM–PVA films are indeed oriented with respect to the directed surface normal.

Discussion

We are now in a position to determine the dipole moment changes upon electronic excitation ($\Delta\mu_{ex}$) and the second-order molecular polarizabilities ($\alpha^{(2)}$) of the bR_{570} and M_{412} interme-

(28) King, G. I.; Schoenborn, B. P. *Methods in Enzymology*; Packer, L. P., Ed.; Academic: New York, 1982; Vol. 88, Part I, p 241.
(29) Earnest, T. N.; Roepe, P.; Braiman, M. S.; Gillespie, J.; Rothschild, K. J. *Biochemistry* **1986**, *25*, 7793.
(30) Clark, N. A.; Rothschild, K. J. *Biophys. J.* **1980**, *31*, 65.
(31) Engelman, D. M.; Henderson, R.; McLachlan, A. D.; Wallace, B. A. *Proc. Natl. Acad. Sci. U.S.A.* **1980**, *4*, 2023.

TABLE II: Nonlinear Optical Properties of *all-trans*-Retinal, Unprotonated Butylamine Schiff Base, Protonated Butylamine Schiff Base, and Bacteriorhodopsin

molecule	oscillator strength[a]	$I(2\omega)/I^2(\omega)$[b]	$\lvert\chi^{(2)}\rvert$[b]	$\alpha^{(2)}_{\zeta\zeta\zeta}$,[c] esu	$\Delta\mu_{ex}/\Delta\mu_{ex}$(ATR)
ATR	0.81 (0.96)	$(7.2 \pm 0.9) \times 10^{-28}$	7.0×10^{-15}	1.5×10^{-28}	1.00 ± 0.12
NRB	0.98 (1.17)	5.1×10^{-28}	5.9×10^{-15}	1.3×10^{-28}	0.85
N^+RB–HCl[d]	0.91 (1.08)	2.5×10^{-27}	1.3×10^{-14}	2.8×10^{-28}	0.74 (0.89)[e]
bR_{570}	0.90 (1.05)	$(5.5 \pm 0.4) \times 10^{-26}$	4.7×10^{-10}	2.5×10^{-27}	1.0 ± 0.1 (1.5)[e]
M_{412}	0.90	6.5×10^{-28}	5.1×10^{-11}	2.8×10^{-28}	1.0

[a] Calculated from the molecular absorption spectra. The action of the solvent was taken into account by using the model B proposed in ref 37. The numbers enclosed in the parentheses are the values before the solvent correction. [b] The reflected p-polarized SH intensity, $I_{s\to p}(2\omega)$, and the second-order surface susceptibility component, $\chi^{(2)}_{xzx}$, were determined for the retinylidene Langmuir–Blodgett monolayers, whereas for the bR_{570} and M_{412} species the transmitted SH beam, $I_{p\to p}(2\omega)$, and $\chi^{(2)}_{zzz}$ were measured in a PM–PVA film. [c] The number density of molecules and the molecular orientational angle away from the film normal are 2.5×10^{14} cm^{-2} and 55° for the Langmuir–Blodgett monolayers. For the PM–PVA film, 7.4×10^{16} cm^{-3} and 30° are the values. [d] The data of this molecule were obtained on a monolayer that was spin-coated onto a glass surface. The absorption maximum is 430 nm, which is about 15 nm blue-shifted from 445 nm observed in methanol. [e] The numbers enclosed in the parentheses are the corrected values where the effect of the resonant damping of the molecules has been taken into account.

diates. Quantum-chemical calculations[32] have demonstrated that upon electronic excitation there is a dramatic charge redistribution from the β-ionone ring to the end group of the retinylidene chromophore. Charge transfer of this type provides a substantial contribution to the second-order molecular polarizability component ($\alpha^{(2)}_{\zeta\zeta\zeta}$) along the charge-transfer direction (ζ). The connection between the second-order nonlinear susceptibility ($\chi^{(2)}$) and the microscopic second-order molecular polarizability ($\alpha^{(2)}$) is given by[22]

$$|\chi^{(2)}_{zzz}| = NL_\omega L_\omega L_{2\omega}\langle\cos^3\zeta\rangle\alpha^{(2)}_{\zeta\zeta\zeta} \qquad (14)$$

where N is the number density of chromophores; L_ω ($L_{2\omega}$) is the Lorentz–Lorentz type local field factor which is given by $(n_\omega^2 + 2)/3$, and the $\langle\ \rangle$ indicates the average over the orientational distribution.

The value of $|\chi^{(2)}_{zzz}|$ can be obtained from the experimentally determined SH intensity, $I_{p\to p}(2\omega)/I_p^2(\omega)$. By use of a 173-μm-thick PM–PVA film with $OD_{566} = 0.1348$, the SH signal at the maximum of the Maker fringe is about 0.31 of that from the quartz crystal. After correcting the self-absorption effect, we obtain a value of $(5.5 \pm 0.4) \times 10^{-26}$ for $I_{p\to p}(2\omega)/I_p^2(\omega)$. Substituting the known values of n_ω, Δn, and $\zeta = 30°$ for PM–PVA films into eq 3, $I_{p\to p}(2\omega)/I_p^2(\omega) = 2.5 \times 10^{-7}|\chi^{(2)}_{zzz}|^2$. This gives a value of $|\chi^{(2)}_{zzz}| = (4.7 \pm 0.2) \times 10^{-10}$ for the unbleached PM–PVA sample. With $N = 7.4 \times 10^{16}$ cm^{-3}, $\zeta = 30°$, and $L_\omega \simeq 1.57$ ($L_{2\omega} = 1.59$), we can further deduce $\alpha^{(2)}_{\zeta\zeta\zeta} = (2.5 \pm 0.2) \times 10^{-27}$ esu for the retinylidene chromophore of the bR_{570} species.

A simple two-level model has been used to derive a connection[33] between $\Delta\mu_{ex}$ and $\alpha^{(2)}_{\zeta\zeta\zeta}$

$$\alpha^{(2)}_{\zeta\zeta\zeta} = \frac{3e^2\hbar^2}{2m_e}\,\frac{\omega_{ng} f \Delta\mu_{ex}}{(\omega_{ng}^2 - 4\hbar^2\omega^2)(\omega_{ng}^2 - \hbar^2\omega^2)} \qquad (15)$$

where ω_{ng} and f are the energy and the oscillator strength of the transition. This equation, however, is valid only for the nonresonant case where the damping constant of the electronic state can be neglected. However, in molecules such as bR_{570} and N^+RB–HCl the damping constant has to be included and then the dipole moment change obtained from $\alpha^{(2)}_{\zeta\zeta\zeta}$ can be expressed as[34]

$$\Delta\mu_{ex}|_{\Gamma_n\neq 0} = \tau\Delta\mu_{ex}|_{\Gamma_n=0} \qquad (16)$$

with

$$1/\tau = (1/6x)[4x_n(4x^2 + x_n^2)(x^2 + x_n^2) + 4(9x^2 + x_n^2) + 8x_n^2(7x^2 + x_n^2)]^{1/2}[(4x^2 - 1)^2(x^2 - 1)^2]^{1/2}/\{[(4x^2 + x_n^2)^2 - 2(4x^2 - x_n^2) + 1][(x^2 + x_n^2)^2 - 2(x^2 - x_n^2) + 1]\}^{1/2}$$

where $x = \omega/\omega_{ng}$ and $x_n = \Gamma_n/\omega_{ng}$. Here τ is a correction factor that takes into account the effect of the damping constant (Γ_n).

Substituting this correction factor into eq 15 yields $\Delta\mu_{ex}|_{\Gamma_n\neq 0} = (F/f)\alpha^{(2)}_{\zeta\zeta\zeta}$. Here F combines the effect of damping with the resonant denominator and the constants in eq 15. In Figure 7, F is plotted as a function of wavelength for NRB (the solid line), N^+RB–HCl (dashed line), and bR_{570} (dotted line) relative to the F of retinal. This allows for the comparison of the induced dipole changes for different molecules using different wavelengths of the exciting fundamental beam.

In this paper (see Table II), the second-order nonlinear optical properties of the free and bound retinylidene chromophores are reported, using a 1.06-μm beam. Previously, we have used a green 532-nm exciting laser beam to investigate free retinal and retinylidene chromophore.[13] The formulas that are used for the analysis of the reflected SH electric fields from monolayers of the free chromophore were derived by Dick et al.[35] The indexes of refraction of monolayers can be taken to be equal to that of the ambient medium (i.e., air).[36] With an s-polarized excitation beam incident on these Langmuir monolayers at a 45° angle of incidence, the equation for the reflected p-polarized SH intensity becomes $I_{s\to p}(2\omega)/I_s^2(\omega) = 14.6|\chi^{(2)}_{xzx}|^2$. The intensities of the reflected SH signals from *all-trans*-retinal (ATR) and NRB monolayers on a water subphase at a surface pressure of 13 dyn/cm are about $(4.8 \pm 0.6) \times 10^{-3}$ and $(3.4 \pm 0.6) \times 10^{-3}$ of the calibrating quartz signal. After calibration with the quartz signal, these measurements give values of $(7.2 \pm 0.9) \times 10^{-28}$ and $(5.1 \pm 0.9) \times 10^{-28}$ cm^2/erg for $I_{s\to p}(2\omega)/I_s^2(\omega)$ of the retinal and NRB Langmuir monolayers, respectively. After transforming to $|\chi^{(2)}_{xzx}|$, the second-order molecular polarizability, $\alpha^{(2)}_{\zeta\zeta\zeta}$, can be estimated from eq 5. The surface density of the monolayer and the inclination angle of the molecule relative to the film normal are chosen to be 2.5×10^{14} cm^{-2} and 55° according to the results of our previous paper.[13] The dipole moment changes can also be obtained from eq 15 with oscillator strengths estimated from the absorption spectra of these two molecules in methanol. The SH data of protonated N^+RB–HCl were obtained from a monolayer that was spin-coated onto a glass surface. The SH signal of the N^+RB–HCl monolayer was about 5 times stronger than that from a similarly prepared unprotonated NRB monolayer. The bound retinylidene chromophore was studied in PM–PVA films as described above. The results for the second-order nonlinear optical properties of the free and bound retinylidene chromophores are summarized in Table II.

Our data of the dipole moment changes depend upon the values of the oscillator strengths. The oscillator strengths are estimated from the absorption spectra of the retinylidene chromophores in solutions. Since two different solvents (water for PM suspension and methanol for the free chromophores) are involved, it is important to remove any solvent effect to reveal the intrinsic properties of the solutes. This is accomplished by using model B proposed by Danilova et al.[37] The dipole moment changes in Table II were deduced with these corrected oscillator strengths.

(32) Birge, R.; Hubbard, L. M. *J. Am. Chem. Soc.* **1980**, *102*, 2195.
(33) Oudar, J. L.; Chemla, D. S. *J. Chem. Phys.* **1977**, *66*, 2664.
(34) Shen, Y. R. *The Principle of Nonlinear Optics*; Wiley: New York, 1984; p 17, eq 2-17.
(35) Dick, B.; Gierulski, A.; Marowsky, G.; Reider, G. A. *Appl. Phys. B* **1985**, *38*, 107.
(36) Guyot-Sionnest, P.; Shen, Y. R.; Heinz, T. F. *Appl. Phys. B* **1987**, *842*, 237.
(37) Danilova, V. N.; Morozova, Yu. P. *Opt. Spectrosc.* **1962**, *12*, 5.

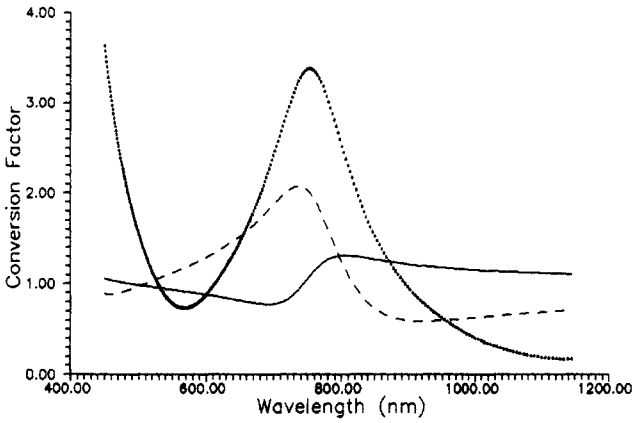

Figure 7. Conversion factor, F, which converts $\alpha^{(2)}_{zzz}$ to $\Delta\mu_{ex}$, is plotted as a function of the wavelength of the exciting fundamental beam. The dotted line represents the calculated result for bR_{570} with the transition energy and damping constant being 2.192 eV and 1200 cm^{-1}. The solid and the dashed lines are for NRB and N^+RB–HCl, respectively. The transition energies for these two molecules are chosen to be 3.399 eV (365 nm) for NRB and 2.885 eV (430 nm) for N^+RB–HCl. The damping constants for both molecules are taken to be 2000 cm^{-1}. All of the curves are normalized relative to F of retinal, whose resonant energy and damping constant are 3.265 eV (380 nm) and 2000 cm^{-1}.

With this procedure the normalized dipole moment changes are insensitive to the absolute magnitudes of the oscillator strengths.

It is interesting to note from Table II that the normalized dipole moment change, $\Delta\mu_{ex}/\Delta\mu_{ex}(N^+RB\text{–}HCl)$, of the retinal chromophore in bR_{570} is about a factor of 1.7 larger than that of the free chromophore. It has previously been suggested[44] that a large change in the chromophore dipole moment upon light absorption could be a crucial step in the excitation mechanism of retinylidene proteins. The results from the SH experiments reported in this paper demonstrate for the first time that such a large change in the chromophore dipole moment does indeed occur in bacteriorhodopsin.

It should be pointed out that SHG with an infrared beam exerts little perturbation on the purple membrane; thus, it can reveal the properties of the purple membrane more directly. This characteristic of SHG is important in the study of such proteins, where the intense electric fields used in the electrochromic methods applied previously to study these dipole changes will polarize the amino acid residues surrounding the chromophore and thus could lead to the reduced response of the chromophore observed by Ponder.[38]

The damping constant, which is needed to calculate the correction factor for dipole moment change in bR_{570}, deserves further comment since the SH frequency is very close to the resonance frequency of the chromophore. The damping constant ($\simeq$1200 cm^{-1}) that is used in this paper for bR_{570} is in close agreement with the results of femtosecond hole burning recently reported.[39] Thus, it is unlikely that there will be any major alteration in the relative values of the induced dipole changes reported here. This is especially true in view of the fact that at 1.06 μm the correction factor, τ, for the free chromophores is relatively insensitive to the damping constant used.

Finally, an additional interesting finding is that the dipole moment change of the retinal chromophore in bR_{570} is larger than that in M_{412}. This result is consistent with the conclusion from resonance Raman spectroscopy of the purple membrane that the chromophore of M_{412} is unprotonated.[40]

Conclusion

In conclusion, we have obtained the second-order nonlinear optical properties of the bacteriorhodopsin molecule in the bR_{570} and M_{412} states. Our results indicate that upon electronic excitation the dipole moment change of the retinal chromophore in bR_{570} is about a factor of 1.7 larger than the free chromophore. Our results also support the notion that the chromophore in the M_{412} intermediate is unprotonated. The experiments described in this paper demonstrate that second-harmonic generation could readily be extended to other relevant biological and chemical applications that require the investigation of dipolar and structural relationships between related membrane systems.

Appendix

Procedure for Calculating the Mole Fractions of the bR Photochemical Intermediates. The main results of this paper, which are summarized in Table II, are based on the conclusion that the observed SH signals from the PM–PVA films originate from the retinylidene chromophore. The data that lead to this conclusion are shown in Figure 3. In this figure, the curves for the mole fractions of bR_{570} and M_{412} are calculated from the bR photochemical cycle shown in Figure 1. For the calculated results in Figure 3 it is important to realize that every intermediate in the photochemical cycle except bR_{570} either can thermally decay into the next subsequent state (shown by the solid arrow) or can be converted to the initial bR_{570} state by absorbing a photon (shown by the dashed arrow).[41] The transition $bR_{570} \rightarrow M_{412}$ is reversible with quantum efficiencies $\psi(bR\rightarrow K) = 0.7$ and $\psi(K\rightarrow bR) = 0.3$.[24] The J_{650} intermediate is neglected because of its much shorter lifetime. For the remaining long-lived photochemical states, the quantum efficiencies for the transitions to the bR_{570} are approximated by 1.

The rate equations for this system become

$$\begin{aligned} dC_R/dt &= I\nu\sigma_K\psi_{KR}C_K - I_\nu\sigma_R\psi_{RK}C_R + I_\nu\sigma_0C_0 + \kappa_0C_0 + \\ &\qquad I_\nu\sigma_NC_N + I_\nu\sigma_MC_M + I_\nu\sigma_LC_L \\ dC_K/dt &= I_\nu\tau_R\psi_{RK}C_R - I_\nu\tau_K\psi_{KR}C_K - \kappa_KC_K \\ dC_L/dt &= \kappa_KC_K - \kappa_LC_L - I_\nu\sigma_LC_L \\ dC_M/dt &= \kappa_LC_L - \kappa_MC_M - I_\nu\sigma_MC_M \\ dC_N/dt &= \kappa_MC_M - \kappa_NC_N - I_\nu\sigma_NC_N \\ dC_0/dt &= \kappa_NC_N - \kappa_0C_0 - I_\nu\sigma_0C_0 \end{aligned} \tag{17}$$

with

$$C_R + C_K + C_L + C_M + C_N + C_0 = 1$$

where I_ν is the intensity of the bleaching light with frequency ν; σ's and κ's are the absorption cross sections and the rate constants of the intermediates. The absorption cross section is related to the extinction coefficient by $\sigma(\nu) = 3.82 \times 10^{-21}\epsilon_\nu$. With the absorption spectra of the bR photochemical intermediates reported by Lozier[42] and the rate constants shown in Figure 2 (κ = (lifetime)$^{-1}$), the steady-state mole fractions for every intermediate can be calculated.

Note that except for M_{412} the rate constants used in the calculation are directly chosen from the results of the kinetic measurement on PM suspended in water.[43] The lifetime of M_{412}, which is known to sensitively depend on the water content of sample,[43] is the only adjustable parameter for the fit to the SH data of a bleached PM–PVA film. For the best fit, a value of 250 ms for M_{412} is required. This value is significantly larger than that for a PM suspension. However, taking into account the water content of our PM–PVA films, this value agrees well with the result of the bR kinetic study reported by Korenstein et al.[43]

Acknowledgment. This research was supported by U.S. Air Force Grant AFOSR-87-0381 and by a contract from the U.S. Army administered by the Letterman Army Institute of Research to A.L.

Registry No. ATR, 116-31-4; NRB, 61769-47-9; N^+RB–HCl, 61769-46-8.

(38) Ponder, M. Ph.D. Thesis, UC Berkeley, 1983.
(39) Mathies, R. A.; Brito Cruz, C. H.; Pollard, W. T.; Shank, C. V. *Science* **1988**, *240*, 777.
(40) Lewis, A.; Spoonhower, J. P.; Bogomolni, R. A.; Lozier, R. H.; Stoeckenius, W. *Proc. Natl. Acad. Sci. U.S.A.* **1974**, *71*, 4462.
(41) Ottolenghi, M. *Adv. Photochem.* **1980**, *12*, 97.
(42) Lozier, R. H.; Bogomolni, R. A.; Stoeckenius, W. *Biophys. J.* **1975**, *15*, 955.
(43) Korenstein, R.; Hess, B. *Methods in Enzymology*; Packer, L. P., Ed.; Academic: New York, 1982; Vol. 88, Part I, p 180.
(44) Lewis, A. *Proc. Natl. Acad. Sci. U.S.A.* **1978**, *75*, 549.